DECONVOLUTION TECHNIQUE TO DETERMINE LOCAL SPRAY DROP SIZE DISTRIBUTIONS – APPLICATION TO HIGH-PRESSURE SWIRL ATOMIZERS.

Stéphane Boyaval and Christophe Dumouchel
UMR 6614 – CORIA – Université et INSA de Rouen
Laboratoire de Thermodynamique
Site Universitaire du Madrillet, B.P.12
76801 Saint Etienne du Rouvray Cedex, France

Abstract
This paper reports the last part of a study on the drop size distribution of sprays produced by high-pressure swirl atomizers dedicated to gasoline direct injection. This last part focuses on the deconvolution of line-of-sight forward diffraction measurements of the spray drop size distribution in order to understand the variation of the mean drop diameter D_{43} in the head of the spray. First, the spatial resolution of the deconvolution technique is improved by developing a continuous deconvolution procedure. Second, this new procedure is applied on a series of four GDI injectors. The results show that the variation of the mean diameter D_{43} in the head of the spray is related to the presence of the pre-spray. Furthermore, the deconvolution technique allowed the determination of the pre-spray drop size distribution. It is found that the pre-spray drops are still a problem in GDI application and that there are very much a function of the injector geometry.

Introduction

This paper reports an investigation on the volume-based drop size distribution of sprays produced by swirl atomizers dedicated to direct-injection spark-ignited engines. Because of the use of high injection pressures to reduce the atomization time, the spatial density of the spray is high. This prevents from classical measurements of spray drop size distribution. In a previous investigation [1], this problem was overcome by combining an experimental approach to the application of the Maximum Entropy Formalism (M.E.F.). The resulting procedure, briefly described hereafter, succeeded in obtaining drop size distribution for a series of four swirl atomizers used at different injection pressures. The behavior of the four injectors was examined under both steady and transient working conditions.

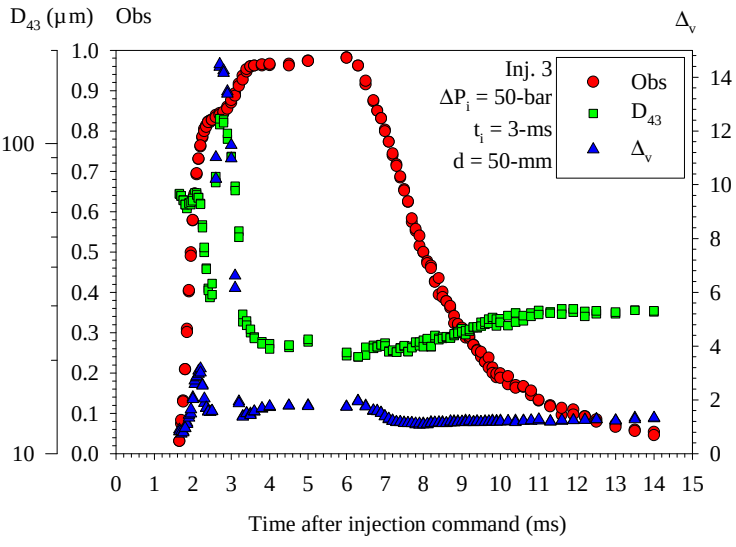

Figure 1. Temporal evolution of *Obs*, D_{43} and Δ_v during one injection.

The experimental part of the procedure made use of the line-of-sight forward-diffraction technique. The effects of multiple light scattering caused by the high spray density were evaluated according to the Obscuration parameter *Obs* given at each measurement. In accordance with previous investigation, it was found that the multiple light scattering effect is non-negligible when *Obs* > 0.6. Furthermore, characteristics of the drop size distributions resulting from the mathematical inversion procedure were then corrected from any multiple light scattering effects. For each working condition, we focused on the determination of the mean drop diameter D_{43} and of the relative span factor Δ_v of the volume-based drop size distribution. A result is presented in Fig. 1 that reports the temporal evolution of *Obs*, D_{43} and Δ_v during one injection, for one injector (Inj.3) used at an injection pressure ΔP_i = 50-bar and an injection time t_i = 3-ms. The measurements were conducted at a distance d = 50-mm from the injector.

The experimental procedure is restricted to the determination of drop size distribution characteristics as presented in Fig. 1 for instance. It does not allow the determination of global drop size distribution. This limitation

was overcome by the application of the Maximum Entropy Formalism (M.E.F.) following a procedure finalized in a previous investigation [2]. The M.E.F. application leads to an analytical expression for the volume-based drop size distribution f_v, namely:

$$f_v(D) = \frac{q^{(q-4)/q}}{\Gamma\left(\frac{4}{q}\right)} \frac{D^3}{D_{q0}^4} exp\left[-\frac{1}{q}\left(\frac{D}{D_{q0}} \right)^q \right] \quad (1)$$

where D represents the drop diameter, Γ, the gamma function, and, q and D_{q0} are two parameters. It was found that the use of the experimental couple of information (D_{43} ; Δ_v) to determine the parameters q and D_{q0} ensures an acceptable description of the volume-based drop size distribution [1, 2].

The reliability of the application of the M.E.F. in the present context was checked for injection pressures up to 70-bar. In each situation the main peak of the distribution was satisfactorily predicted and a good description of the big drop population was observed. Therefore, the M.E.F. distribution ensures a good estimation of the maximum drop diameter. This latter information is of paramount importance in G.D.I. application since the drops should not exceed 50-µm in diameter [3].

The investigation summarized above reports drop size distribution spatially integrated along a diameter of the spray. The purpose of the present study is to determine local drop size distributions to have a better information on the position of the big particles in the spray. This is achieved by applying a deconvolution technique allowing the determination of local information from space integrated measurements.

The deconvolution procedure

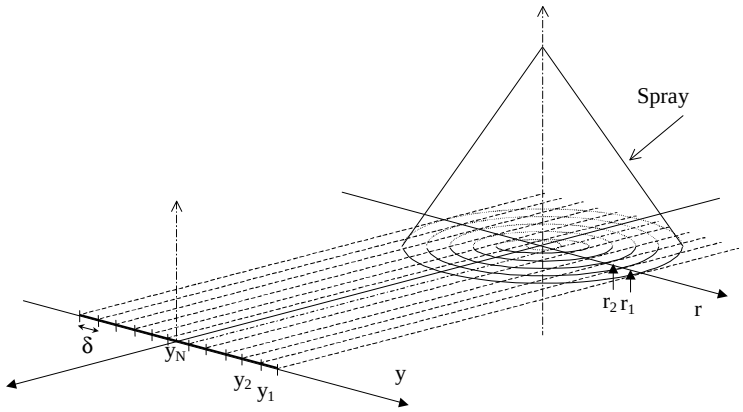

Figure 2. Description of the deconvolution procedure.

The deconvolution technique allows the conversion of line-of-sight averaged drop size distribution into spatially resolved information. As a first step, the classical procedure described in the literature for similar situations is applied [4, 5, 6]. This technique requires that the drop size distribution of the spray is axisymmetric. It was shown that sprays produced by high-pressure swirl atomizers satisfy this assumption [1]. The spray can be divided into annular rings as shown in Fig. 2, each ring being characterized by a local drop size distribution that we want to determine. To achieve this, a series of N measurements is performed, each measurement corresponding to a given position y_i of the laser beam (see Fig. 2): y_1 is the external position and y_N is the central position where the measurement is conducted along a diameter of the spray. The distance between each consecutive position ($y_i - y_{i+1}$) is equal to the width δ of the laser beam. The series of 31 intensities $I_j(y_i)$ collected on the 31 diodes at each measurement are corrected from multiple light scattering effects using correction factor series established for each diode according to the obscuration [1]. For 5 diodes among the 31, Fig. 3 presents the correction factor series versus *Obs* (diode 31 is the external diode). As said in the introduction, it can be seen in this figure that the multiple light scattering has a reduced effect when the Obscuration parameter is less than 0.6.

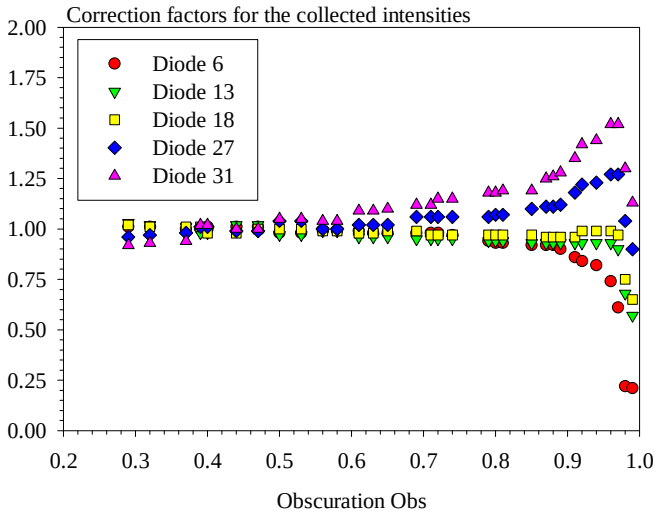

Figure 3. Correction factors for the collected intensity versus the Obscuration. Influence of the diode [1].

The deconvolution procedure is applied on the corrected intensity series $I_j(y_i)$ to determine the intensity per unit length series $I_j(r_k)$. Using the classical formulation, the two intensity series are related by:

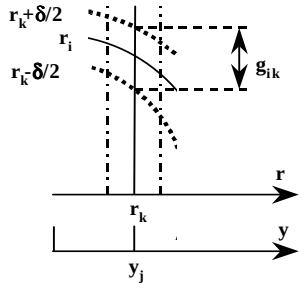

Figure 4. Definition of the coefficients g_{ik}.

$$I_j(y_i) = 2\sum_{k=1}^{i} g_{ik} I_j(r_k) \qquad i = 1 \text{ to } N,\ j = 1 \text{ to } 31 \tag{2}$$

where the coefficients g_{ik}, defined in Fig. 4, are given by:

$$g_{ik} = \sqrt{\left(r_k + \frac{\delta}{2}\right)^2 - r_i^2} - \sum_{m=k+1}^{i} g_{im} \tag{3}$$

For each ring, defined by a radial position r_k, a series of 31 intensities $I_j(r_k)$ is available and can be sent to the inversion procedure of the instrument to get a local volume-based drop size distribution and its characteristics. The spatial resolution of the deconvolution procedure is equal to the diameter of the laser beam used to perform the measurement. In our case this diameter is equal to 8-mm. Reducing the laser beam diameter can increase the accuracy of the deconvolution procedure. We did not have the opportunity to do so and we decided to reconsider the previous procedure in order to develop a continuous deconvolution technique.

The continuous deconvolution technique is identical to the classical method except that the number of measurements N is increased and the radial shift between each measurement is reduced. This radial shift is now equal to δ/p where the step p is an even number. Figure 5 shows the position of the measurements for a step $p = 2$. It can be shown that the equation system (2) takes now the form:

$$\begin{cases} I_j(y_i) = \sum_{k=i}^{i+p-1} G_j(r_k) & \text{for } 1 \le i \le N - \frac{p}{2} \\ I_j(y_i) = \sum_{k=i}^{2N-i-1} G_j(r_k) + 2\sum_{k=2N-i}^{N+\frac{p}{2}-1} G_j(r_k) & \text{for } N - \frac{p}{2} + 1 \le i \le N \end{cases} \tag{4}$$

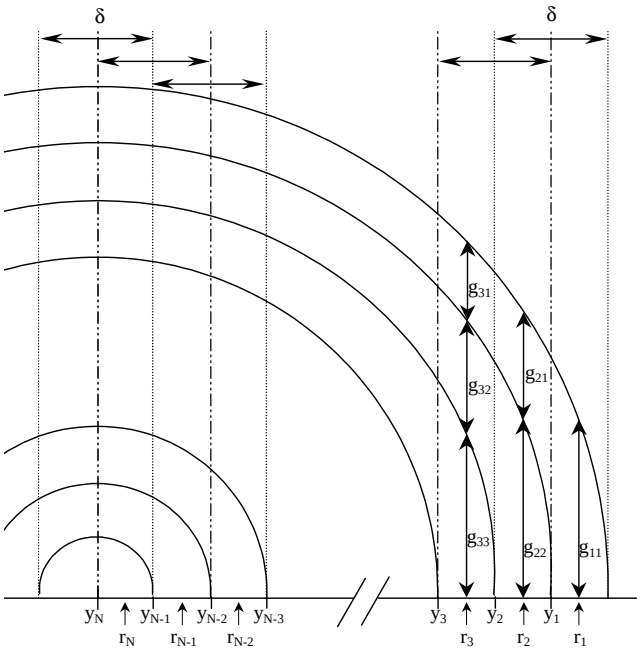

Figure 5. Position of the measurements for a step $p = 2$.

where the functions G_j are given by:

$$G_j(r_i) = 2\sum_{k=1}^{i} g_{ik} I_j(r_k) \tag{5}$$

As in the previous situation, the resolution of the equation system (4) allows to determine series of local intensities $I_j(r_k)$ that are introduced in the mathematical inversion procedure to calculate the volume-based drop size distribution. The equation system (4) leaves us with a problem. Indeed, according to the last term of the second equation of system (4), the number of radial positions involved in the procedure is equal to $N+p/2-1$. When the step p is greater than 2, this number is higher than the number of available measurements, i.e., N. Thus a number of $p/2-1$ supplementary equations is required to close the system. This problem can be avoided if the step p is not greater than 2. This is why we decided to limit the application of the continuous deconvolution procedure with a step $p = 2$. In the present context, the highest accuracy of the deconvolution procedure is equal to 4-mm (half of the laser beam diameter). Finally, despite the fact that the deconvolution procedure allows the determination of local volume-based drop size distribution, it was preferred in the following to concentrate on the experimental determination of the mean drop diameter D_{43} and of the relative span factor Δ_v. The reason for this is that the correction performed on the intensities may lead to unrealistic representation of the small drop population. An example is presented in Fig. 6 that shows the volume-based drop size distribution obtained for Inj. 2 used at 65-bar. It can be observed that the small drop population is not physical. The determination of the two parameters D_{43} and Δ_v is believed to be of much better quality and allows the reconstruction of the volume-based drop size

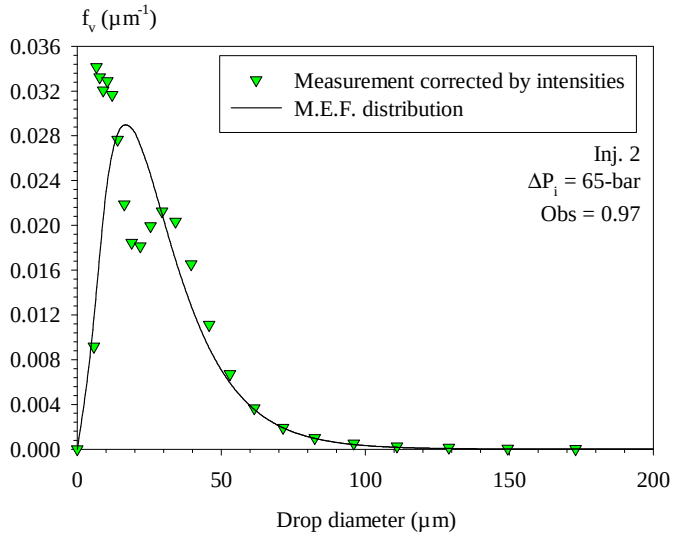

Figure 6. Comparison between a measured and a calculated drop size distribution (Inj. 2, ΔP_i = 65-bar, *Obs* = 0.97).

Injector	Δ'	Δ''
Inj. 1	1.92	1.0
Inj. 2	1.92	0.5
Inj. 3	1.18	1.0
Inj. 4	1.18	0.5

Table 1. Shape parameters of the four injectors.

distributions from the application of the mathematical distribution issued from the application of the M.E.F. (Eq. [1]). Figure 6 shows the M.E.F. distribution. It can be seen that the representation of the big drop population is in accordance to the experimental result.

The deconvolution procedure presented in this paper was applied on a series of four high-pressure swirl atomizers dedicated to GDI. These injectors are those studied in a previous investigation [1]. They differ from their internal geometrical characteristics as indicated in table 1 that presents the shape parameters Δ' and Δ'' introduced by Dombrowski and Hasson [7] to characterize swirl injector behavior. All the measurements presented in this paper were performed 50-mm far from the injector.

Results

One of the main objectives of the present work is to understand the maximum D_{43} observed in each situation in the head of the spray. An example of this maximum can be seen in Fig. 1 where D_{43} reaches a value greater than 100-µm 2.7-ms after the injection command. It was suspected that this maximum is due to the presence of the pre-spray. Injected at the very beginning of the injection, the pre-spray is composed of liquid having no rotational momentum and penetrates the gas environment with a great axial velocity compared to the fully developed flow. Pre-sprays are known to mainly contain the biggest drops of the spray. Furthermore it has often been reported that pre-sprays drastically increase the penetration length of the spray. For the four injectors studied here, it can be seen in Fig. 7 that the pre-spray does not induce extended penetration length. The pre-spray drops have a small velocity and are rapidly overtaken by smaller drops produced slightly later and belonging to the main spray body. The pre-spray drops take more time than the drops of the front edge of the spray to reach the location where the drop size distribution measurement is performed.

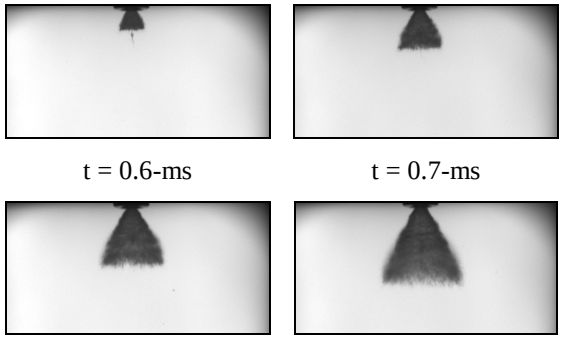

Figure 7. Beginning of the injection (Inj. 3, ΔP_i = 70-bar, t_i = 3-ms, f = 20-Hz).

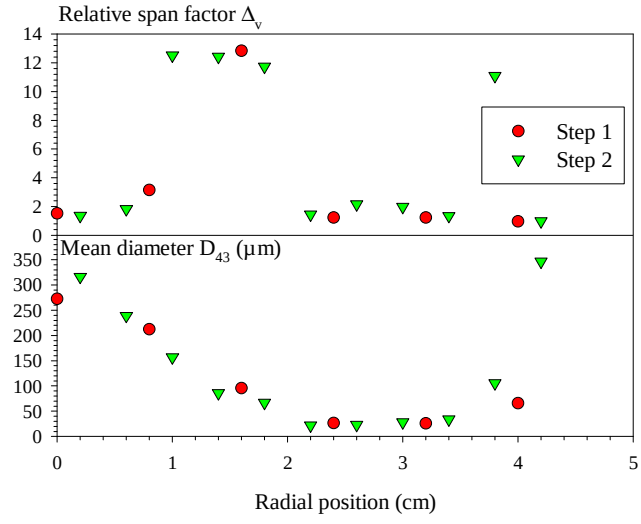

Figure 8. Radial evolution of the mean diameter D_{43} and of the relative span factor Δ_v. Inj. 3, ΔP_i = 50-bar, 2.7-ms after the injection command.

The application of the deconvolution procedure should confirm this result. This is why we decided to apply the deconvolution procedure for the sprays reporting the maximum D_{43} in the spray head. For each injector used at an injection pressure of 50-bar, the series of measurements required for the procedure was conducted at the time after the injection command where the maximum D_{43} was observed [1]. For the step p = 1, the number of measurements N was equal to 6 to cover the all spray. With p = 2, this number becomes equal to 11. All the measurements were performed at 50-mm

from the injector.

Figure 8 presents the results of the deconvolution procedure performed with Inj. 3. This figure shows the local characteristics D_{43} and Δ_v obtained either with a step equal to 1 and 2. It must be first observed that globally speaking, the results obtained for the two steps are in good agreement. For both distribution characteristics, a unique radial evolution is found. However, one should note that the results reported in the outskirts of the spray show some differences. Indeed, with a step equal to 2, an increase of the mean diameter D_{43} is observed when the outskirts of the spray are approached. This behavior is accompanied by a peak in Δ_v at the position 3.8-mm. Such results are not obtained when the deconvolution procedure is conducted with a step p = 1. It is difficult here to claim that the benefit of accuracy due to an increase of the step parameter allows the observation of behavior hidden when the analysis is conducted with a smaller step. However, one should add here that many different investigations found in the literature [8, 9, 10] reported the presence of big drops in the outskirts of the spray and mainly during the first stage of the injection.

Figure 8 indicates also that the mean drop diameter D_{43} increases as the axis of the spray is approached and reaches a maximum at r = 0-cm. This confirms that the maximum D_{43} reported in the head of the spray is due to the presence of big particles located on the axis. These particles are of course those that constitute the pre-spray.

As explained in the previous section, the mathematical distribution issued from the application of the M.E.F. and given by Eq. (1) can be used to represent the global volume-based drop size distribution. The relevance of the use of this mathematical function was discussed in detail in [1] and can be appreciated in Fig. 6. Although they are some discrepancies, it must be kept in mind that the big drop population, i.e. the tail of the distribution, is usually well reproduced by the mathematical distribution. The application of the mathematical distribution was fully detailed in [2]. It requires the knowledge of the characteristics D_{43} and Δ_v for the determination of the parameters q and D_{q0}. The results presented in Fig. 8 were used to determine the local drop size distributions of the spray produced by Inj. 3, 2.7-ms after the injection command and at 50-mm from the injector. These distributions, presented in Fig. 9, were calculated for the deconvolution step equal to 2 which offers the determination of a volume-based drop size distribution each 4-mm.

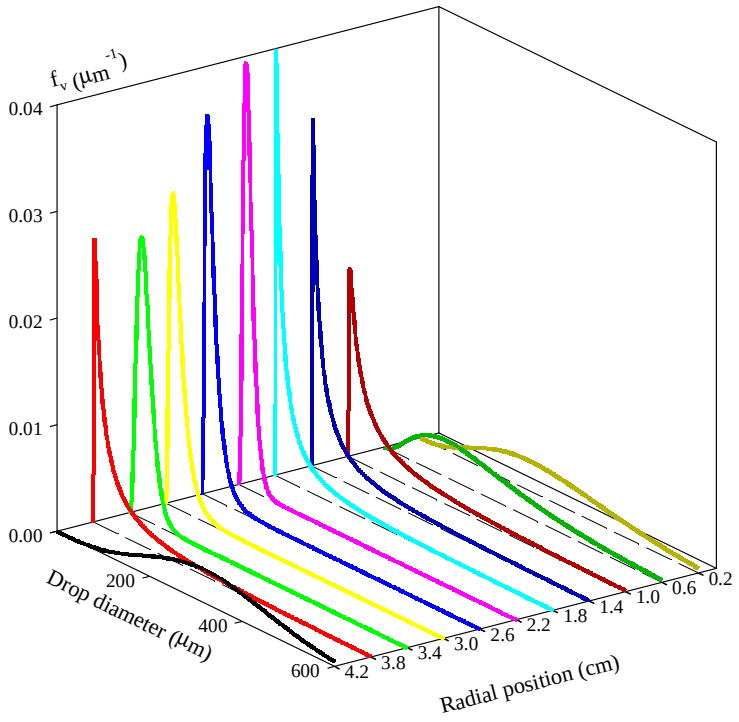

Figure 9. Local volume-based drop size distribution. . Inj. 3, ΔP_i = 50-bar, 2.7-ms after the injection command. Deconvolution step: 2.

The series of drop size distribution presented in Fig. 9 reports a clear dependence between the size of the particles and their position. Considering the fact that the M.E.F. distribution offers a rather good description of the big drop population, we concentrate on this very population. It can be seen in Fig. 9 that the large drops are located either in the outskirts of the spray or in the center, confirming what was observed in Fig. 8. As said above, the presence of large drops in the outskirts of the spray was reported by experimental investigations found in the literature. These drops are probably produced right at the beginning of the atomization process and keep a ballistic trajectory because of their size.

As suspected, the biggest drops of the spray evolve in the center. This location confirms that these drops belong to the pre-spray and that the maximum D_{43} reported during the first injection stage is well related to the presence of a low velocity pre-spray. The pre-spray contains very large drop. Indeed, the distribution obtained at 0.2-cm spread above 600-µm. Studying GDI swirl injector showing an extended pre-spray, Parrish and Farrel [8], reported in comparable working condition (ΔP_i = 48.3-bar) a pre-spray with a mean diameter D_{32} not greater than 60-µm. This difference can be explained by considering the velocity of the pre-spray. In Parrish and Farrell study, the pre-spray velocity was higher than the main spray velocity. In the present case, this is the opposite. As far as the penetration length is concerned, the present injectors are better than those studied by Parrish and Farrell since they induce no extended penetration length (see Fig. 7). However, considering the degree of atomization of the pre-spray, the injectors studied by Parrish and Farrell showed a better efficiency: it is known that the higher the velocity, the higher the degree of atomization.

In consequence, the pre-spray drop size distribution is still an important problem in GDI application. The pre-spray drop size distribution is a function of the internal geometry of the injector. This is presented in Fig. 10 that shows the pre-spray drop size distribution for the four injectors. The injection pressure is ΔP_i =50-bar. Generally speaking we can see that the injectors with the largest shape parameter Δ' (Inj. 1 and 2) produce a better atomized pre-spray. It is important to add here that these very injector are those that produce less atomized sprays in the fully open conditions, i.e., in the main spray body [1]. This last remark shows the trickiness of the pre-spray problem.

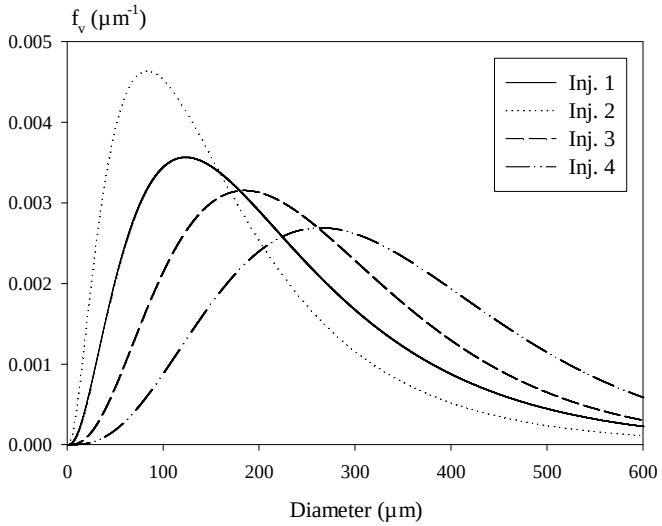

Figure 10. Influence of the injector geometry on the pre-spray drop size distribution.

Conclusion

The work reported in this paper presents a method to improve the spatial resolution of the deconvolution procedure applied on space integrated spray drop size distributions. These distributions are obtained from a line-of-sight forward diffraction technique. The deconvolution procedure allows the transformation of the measurements into local information. In classical deconvolution procedure, the spatial resolution is equal to the laser beam diameter. To improve the accuracy, one has to reduce the diameter of the laser beam. In the present study we suggested another method to increase the accuracy of the procedure without any modification of the instrument. Theoretically speaking, this new method allows reaching a high degree of spatial resolution. Indeed the spatial resolution of the procedure is now given by the radial shift between two consecutive measurements, shift that can be reduced without any limitation. This is why this technique was called the continuous deconvolution technique. This new deconvolution technique was applied on a series of four GDI high-pressure swirl injectors. This allowed understanding that the variation of the mean diameter D_{43} in the first injection stage is due to the passage of the pre-spray in the measuring volume. Thus, it was possible to determine the pre-spray drop size distribution and to show the influence of the injector geometry on this characteristic. It was found that the pre-spray drops are much bigger when the pre-spray is very slow. In GDI application this constitutes an advantage as far as the penetration length is concerned. However, the poor atomization quality might be an important problem. It was found also that the pre-spray drop size distribution is a function of the injector geometry: the injectors with the best atomization efficiency in fully open condition are those producing bigger pre-spray drops. This result shows that the pre-spray is still an important and very tricky problem in GDI application

References

[1] Boyaval, S., and Dumouchel, C., *Part. Part. Syst. Char.* 18, 33-49 (2001)
[2] Dumouchel, C., and Boyaval, S., *Part. Part. Syst. Char.* 16, 177-184 (1999)
[3] Zhao, F.Q., Lai, M.C., Harrington, D.L., *SAE Technical Paper* n°970627, (1997)
[4] Gomi, H., Thesis, University of Sheffield, December 1984
[5] Yule, A., Ah Seng, C., Felton, P.G., Ungut, A., Chigier, N.A., *Symposium (International) on Combustion, The Combustion Institute*, 1981, pp.1501-1510
[6] Dodge, L.G., Rhodes, D.J., Reitz, F.D., *Applied Optics* 16, 2144-2154 (1987)
[7] Dombrowski, N., and Hasson, D., *AIChE J.* 15, 604-611 (1969)
[8] Parrish, S.E., Farrell, P.V., *SAE technical Paper* n°970629, (1997)
[9] Xu, M., Markle, L.E., *SAE Technical Paper* n°980493, (1998)
[10] Yoo, J.H., Zhao, F.Q., Liu, Y., Lai, M.C., Lee, *Eighth International Conference on Liquid Atomization and Spray Systems*, Pasadena, USA, July 2000, pp.498-505.